Full Length Article

¹H NMR-Based Metabolomics to Identify Resistance-Related Metabolites in *Astragalus membranaceus* var. *mongholicus* against *Fusarium* Root Rot

Fen Gao[1*], Jianbin Chao[2], Jie Guo[3], Li Zhao[4] and Haijiao Tian[3]

[1]*Institute of Applied Chemistry, Shanxi University, Taiyuan 030006, P. R. China*
[2]*Scientific Instrument Center, Shanxi University, Taiyuan 030006, P. R. China*
[3]*Shanxi Province Science and Technology Resources and Large Instruments Open Sharing Center, Taiyuan 030006, P. R. China*
[4]*Modern Research Center for Traditional Chinese Medicine, Shanxi University, Taiyuan 030006, P. R. China*
*For correspondence: gaofen@sxu.edu.cn

Abstract

Root rot is a destructive disease of *Astragalus membranaceus* var. *mongholicus* (AMM) and occurs frequently in recent years in the main cultivation regions in China. However, the progress of AMM resistance breeding is extremely slow due to the lack of resistance source and inefficiency of the conventional disease resistance evaluation method. This study aimed to provide information on the interaction between AMM and *Fusarium solani*, one of the predominant pathogens causing root rot and identify the resistance-related (RR) metabolites by using the nontargeted ¹H nuclear magnetic resonance (NMR) metabolomics approach. Of the 24 metabolites examined, the concentration changes in sucrose, fructose, taurine and phenylalanine were negatively correlated with the root rot severity. The abundance of malic acid in *F. solani*-inoculated samples considerably decreased at 21 days post inoculation (dpi). The five metabolites were identified as RR metabolites, and only malic acid inhibited the fungal growth. These metabolites might serve as candidate biomarkers for discriminating the resistance levels of different AMM genotypes and establishing the high-throughput screening method of AMM breeding lines against root rot caused by *F. solani*. Results could assist in accelerating the resistance breeding program. The possible mechanisms of RR metabolites in plant defense against the pathogen were discussed. © 2021 Friends Science Publishers

Keywords: *Astragalus membranaceus* var. *mongholicus*; Biomarker; *Fusarium solani*; Metabolomics; Nuclear magnetic resonance; Resistance-related metabolite

Introduction

Astragali Radix, known as Huangqi in China, is the dried root of *Astragalus membranaceus* var. *mongholicus* (AMM) or *A. membranaceus*. As a traditional folk medicine, AMM is used extensively in medical treatment in Asia particularly in China, Korea, Japan, Mongolia and Siberia for its many pharmacological properties (Li *et al.* 2017). The root rot of this plant is caused by several *Fusarium* species and *F. solani* is of great relevance to it in the main AMM-growing regions in China, including Shanxi, Gansu and Inner Mongolia (Gao *et al.* 2018). As a destructive and devastating disease of AMM, the root rot epidemic leads to considerable economic losses on the part of growers and threatens the production and clinical medication of traditional Chinese medicine. Some agricultural practices, such as application of fungicides and biological control agents or crop rotation, can decrease the disease severity to some extent but have not been entirely effective (Ma *et al.* 2019).

Resistance breeding is an economical and environmentally safe way to manage the diseases (Iqbal *et al.* 2013). However, disease-resistant cultivars have not played their anticipated role in soil-borne disease control in agricultural production because few effective resistance sources against most of the soil-borne diseases of crop, horticultural and medicinal plants have been found. The predominant soil-borne diseases are caused by necrotrophic pathogens, which have competitive saprophytic ability (Li *et al.* 2011). For the AMM root rot, the progress of resistance breeding is extremely slow. To date, only a few cultivars with improved resistance to root rot have been developed. These cultivars are selected on the basis of low disease severity in terms of simple disease ratings and without prior knowledge of mechanisms involved in resistance (Ma *et al.* 2019). In recent years, the germplasm intermixing between cultivated AMM cultivars, which account for more than 80% of the total amount of Astragali Radix, has occurred due to the introduction of seeds from different places and

shortened growth period (Qin *et al.* 2016). This condition makes the selection of the resistance source difficult. Besides, AMM takes approximately three years to complete a normal life cycle, and breeding a cultivar takes 27 years (Ma *et al.* 2019). The conventional disease resistance evaluation method, with disease severity as the evaluation indicator, has low efficiency and long cycle. Thus, breeding a resistant AMM cultivar successfully takes years. The top priority in AMM breeding for resistance against root rot is the development of a high-throughput screening method on the basis of efficient biomarkers. These biomarkers can be applied to discriminate the resistance level of different AMM genotypes or breeding lines. This condition meets the requirements of extensive screening of resistance sources available to the breeder and is favorable for the fast development of root rot resistance breeding in AMM.

Metabolomics, a comprehensive and nonbiased analysis method of metabolite mixtures, is theoretically available for the identification and quantification of every individual metabolite. With the help of metabolomics approach based on nuclear magnetic resonance (NMR), liquid chromatography-mass spectrometry (LC-MS) and gas chromatography-mass spectrometry (GC-MS), a large set of differential metabolites is identified in the process of deciphering the host-pathogen interaction mechanism. These metabolites with significantly higher concentrations in the resistant genotypes than in the susceptible ones were referred to as resistance-related (RR) metabolites (Gauthier *et al.* 2015). Some of these metabolites serve as resistance biomarkers for discriminating the resistance levels in different plant species to various pathogens. More than 340 various metabolites involved in the biochemical defense are identified in *F. graminearum*-wheat/barley pathosystems through the achievement of metabolomics studies. Among these metabolites, jasmonic acid, methyl jasmonate, linolenic acid, linoleic acid, *p*-coumaric acid, caffeyl alcohol, naringenin, catechin, quercetin, kaempferol glucoside and catechol glucoside are considered as biomarkers for discriminating the resistance levels in wheat/barley genotypes and the high-throughput screening of breeding lines (Hamzehzarghani *et al.* 2008; Bollina *et al.* 2010, 2011; Kumaraswamy *et al.* 2011a, b). Thus, metabolomics can facilitate the understanding of resistance mechanisms controlled by metabolites and can be used to identify the metabolic biomarkers for the evaluation of disease resistance. However, no study concerning the use of metabolomics is conducted to elaborate the mechanisms behind the AMM resistance to root rot pathogen and identify RR metabolites as resistance metabolic criteria.

Our study focuses on a time-series metabolic profiling of AMM during *F. solani* infection and disease development through the nontargeted ¹H NMR-based metabolomics. This study is designed to provide information for elucidating resistant mechanisms and identify a series of RR metabolites as resistance biomarkers for the discrimination of the resistance levels of different AMM genotypes and the establishment of a high-throughput screening method of AMM breeding lines against root rot. This study will help accelerate the AMM resistance breeding program to achieve an economical and environment-friendly management of the root rot.

Materials and Methods

Plant and fungal culture

AMM seedlings without any disease-related symptom (1-year-old, root = 0.5–0.6 cm × 10–15 cm) were collected from the planting base in Ningwu County, Shanxi Province, China. Five-day-old cultures of *F. solani* (Gao *et al.* 2018) on potato dextrose agar plates were used to make mycelial disks with 5 mm diameter. Four *F. solani* disks were cultured in potato dextrose liquid medium with shaking at 180 rpm and 25°C for 48 h. The liquid culture was filtered through two layers of cheesecloth and conidial suspension was adjusted to $1.0–1.5 \times 10^6$ conidia mL^{-1} by using a hemocytometer.

Inoculation, incubation and disease severity assessment

Clean AMM roots were soaked in 70% alcohol for 10–15 s and washed for 2–3 times with sterile water. Roots were soaked in the conidial suspension of *F. solani* for 30 min after stabbing with sterile dissecting needles to form wounds (10 spots per root). After inoculation, all the seedlings were grown in 15 cm pots containing pasteurized soil and maintained in a growth room (25°C ± 3°C). The root rot severity (RRS) was determined using the disease index (DI). The rating class was recorded on a scale of 0–4 (0, no visible lesions or mostly no visible lesions; 1, slightly brown lesions and the diameter of lesion site $(D) \leq 2$ mm; 2, moderately brown lesions and 2 mm $< D \leq 3$ mm; 3, extensively dark brown lesions and 3 mm $< D \leq 4$ mm; and 4, whole plant diseased).

Metabolite extraction and NMR analysis

This study adopted the extraction procedures used by He *et al.* (2013) and Li *et al.* (2015). The ¹H NMR spectra of aqueous methanol fraction extracts were recorded at 25°C on the Bruker 600-MHz AVANCE III HD NMR spectrometer (600.13 MHz proton frequency; Bruker BioSpin, Karlsruhe, Germany). CD₃OD was used for internal lock purposes. Each ¹H NMR spectrum consisted of 64 scans requiring 5 min acquisition time with the following parameters: 0.188 Hz per point, pulse width = 30° (12.7 μs), and relaxation delay = 5.0 s (He *et al.* 2013; Li *et al.* 2017). A presaturation sequence (noesygpprld) was used to suppress the residual H₂O signal with low power selective irradiation at the H₂O frequency during the recycle delay. The resulting spectra were manually phased, subjected to baseline correction, and calibrated to TSP at 0.00 ppm.

NMR data processing

The ^{1}H NMR spectra were processed on the MestReNova (version 8.0.1, Mestrelab Research, Santiago de Compostella, Spain) and divided into integrated regions of equal width (0.04 ppm) corresponding to the region of δ 0.20–8.60. The regions of δ 4.70–5.02 and δ 3.30–3.38 were removed from the analysis because of undesired signal caused by residual H_2O and CD_3OD, respectively. The remaining signals were assigned by comparison with the chemical shift of standard compounds through the Chenomx NMR suite of software (Chenomx Inc., Edmonton, AB, Canada, evaluated) and in accordance with the reported data in literature (He *et al.* 2013; Li *et al.* 2015, 2017). These signals were confirmed using the Biological Magnetic Resonance Data Bank (https://bmrb.io/) and the Human Metabolome Database (https://hmdb.ca/). The metabolites were relatively quantified on the basis of the integrated regions from the least overlapping NMR signals of metabolites.

Experimental design and statistical data analysis

The experiment was conducted as a pot culture designed using 2 treatments (inoculated with *F. solani* and mock/sterile water) and 8 replicates. Each replicate consisted of 10 AMM plants. The complete roots of 10 plants were harvested as samples at 0-, 7-, 14- and 21-days post inoculation (dpi), immediately snap-frozen with liquid nitrogen and stored at −80°C for metabolite extraction and NMR analysis.

The preprocessed NMR data were imported into the SIMCA-P software (version 14.1, Umetrics, Umeå, Sweden) for principal component analysis (PCA) and orthogonal projections to latent structures discriminant analysis (OPLS-DA) to discriminate the relationship between metabolite profiles in *F. solani*- and mock-inoculated samples and identify the contribution of individual metabolites to the difference between two treatments. Analysis of variance (ANOVA) was conducted for each measurement of metabolite on the SAS version 9.4 (SAS Institute Inc. Cary, NC, USA) with replications as random factors and inoculation treatments as fixed effects. The metabolite means in *F. solani*- and mock-inoculated samples were separated using the fisher's least significant difference (LSD) test at a probability level of $P < 0.05$. LSD was also used in identifying the statistically significant differences in metabolite concentrations at different sampling times, and the T-test was conducted between *F. solani*- and mock-inoculated samples at each time point. The concentration change was derived from investigating the ratio of change in the mean peak area (normalized intensity value) of each metabolite between *F. solani*- and mock-inoculated samples at each time point. The formula is expressed as follows:

$$Cr\ (\%) = \frac{A - B}{B} \times 100$$

Where Cr is the ratio of concentration change; A and B represents the concentration in treatment and the concentration in control, respectively. The Pearson linear correlation was used to determine the relationships between the concentration changes in metabolites and RRS and identify the metabolites that were highly correlated with the disease severity during the infection of the pathogen.

Identification of RR and pathogenesis-related (PR) metabolites

RR and PR metabolites were identified in accordance with the following criteria. (1) A metabolite was considered an RR metabolite when its concentration changes in *F. solani*-inoculated samples showed evidently negative correlation with RRS or when it had significantly lower abundance in *F. solani*-inoculated samples than in mock-inoculated samples. (2) A metabolite was considered a PR metabolite when its concentration changes in *F. solani*-inoculated samples showed evidently positive correlation with RRS or when it had significantly higher abundance in *F. solani*- than in mock-inoculated samples. These criteria were established based on the criteria proposed by Bollina *et al.* (2010) and Kumaraswamy *et al.* (2011b) and several reports on the timing and extent of host metabolic changes to which fungal infection made a major contribution at the stage of the culture process (Jones *et al.* 2011; Cuperlovic-Culf *et al.* 2016). In addition to the two criteria, the possible action mechanism of a metabolite involved in disease resistance was considered when determining a RR or PR metabolite.

F. solani growth on minimal media

Minimal media were prepared in accordance with the description of Botanga *et al.* (2012). Following autoclaving, filter-sterilized compounds were added to test the ability of *F. solani* to utilize various compounds as carbon source. Sterile water and glucose were used as negative and positive controls, respectively. The medium was supplemented with glucose (1%) and any one of the compounds (20 m*M*) to test the effect of individual metabolite on fungal growth; as control, only glucose (1%). Plates were inoculated with *F. solani* by placing four 5 μL droplets of conidial suspension $(1.0–1.5 \times 10^6$ conidia $mL^{-1})$ and incubated for 72 h at 25°C $\pm$ 1°C and the diameters of colonies were measured.

Results

Disease development

Root rot symptoms developed in all *F. solani*-inoculated roots. Light brown spots occurred at the inoculation site at 7 dpi. The color of the spots gradually deepened, and the size of the lesions increased with time. The inoculation site in control samples became slightly dark but showed no sign of root rot during the culture process. The DIs of *F. solani*-inoculated samples were 0, 20, 65 and 88.16 at 0, 7, 14 and 21 dpi.

Table 1: Chemical shift assignments in aqueous methanol fraction extract of *Astragalus membranaceus* var. *mongholicus* roots

No.	Metabolite	Selected characteristic signals in NMR
1	Valine	1.01 (d, 7.0), 1.06 (d, 7.0)
2	Threonine	1.33 (d, 6.6)
3	Alanine	1.48 (d, 7.2)
4	Arginine	1.68 (m), 1.74 (m), 1.90 (m), 3.24 (t, 7.2), 3.75 (t)
5	Acetic acid	1.94 (s)
6	Glutamine	2.14 (m), 2.46 (m)
7	Glutamate	2.14 (m), 2.46 (m), 4.9(s)
8	Gamma aminobutyric acid	2.30 (t, 7.2), 3.01 (t, 7.2)
9	Malic acid	2.41(dd, 15.3, 9.3), 2.70 (dd, 15.6, 3.4), 4.29 (dd, 9.1, 3.3)
10	Succinic acid	2.45 (s)
11	Citric acid	2.54 (d, 16.7), 2.72 (d, 16.7)
12	Aspartate	2.83 (dd, 16.9, 8.1), 2.95 (dd, 16.9, 4.0)
13	Choline	3.22 (s)
14	Taurine	3.24 (t), 3.44 (t), 3.54 (s)
15	Phenylalanine	3.44 (t, 9.6), 7.33 (m)
16	Fructose	4.20 (d,8.0)
17	*â*-Glucose	4.59 (d, 7.9)
18	*á*-Glucose	5.20 (d, 3.8)
19	Maltose	5.26 (d, 3.7)
20	Sucrose	5.41 (d, 3.8)
21	Fumaric acid	6.53 (s)
22	Adenine	8.22 (s) , 8.28 (s)
23	Formic acid	8.47 (s)
24	Astragaloside	0.34 (m), 0.55 (m)
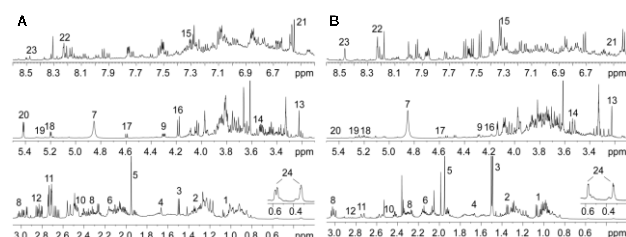
Fig. 1: The typical annotated ^{1}H NMR spectra of the aqueous methanol fraction extracts in mock- (**A**) and in *F. solani*-inoculated (**B**) *Astragalus membranaceus* var. *mongholicus* roots at 21 dpi

Metabolic profiling and metabolite identification

The ^{1}H NMR spectra of mock- and *F. solani*-inoculated AMM roots were divided into three distinct regions (*i.e.*, *A*: δ 1.0–3.5, *B*: δ 3.5–5.5 and *C*: δ 5.5–8.5) and represented by high concentrations of primary metabolites, including amino acids, sugars and organic acids and a few other compounds (Fig. 1). The assignments of major identified metabolites are shown in Table 1. These metabolites were amino acids, *i.e.*, alanine (Ala), arginine (Arg), aspartate (Asp), glutamate (Glu), glutamine (Gln), phenylalanine (Phe), threonine (Thr) and valine (Val); sugars, *i.e.*, fructose, α-glucose, β-glucose, maltose, sucrose; and organic acids, *i.e.*, taurine and acetic, citric, formic, fumaric, gamma aminobutyric (GABA), malic and succinic acids. Choline metabolites (*i.e.*, choline), nucleotide metabolites (*i.e.*, adenine) and astragaloside were also detected.

Multivariate statistical analysis and differential metabolites

PCA was performed to compare the bucketed ^{1}H NMR spectra of the mock- and *F. solani*-inoculated samples and learn the biochemical response of AMM to pathogen challenge. On PCA score plots, the mock-inoculated samples collected at 0, 7, 14 and 21 dpi were clustered together. However, *F. solani*-inoculated samples gradually showed some groupings in terms of post infection time. The differences in independent clusters formed on the PCA score plots indicated that evident biochemical perturbation of metabolites in samples inoculated with *F. solani*. *F. solani*- and mock-inoculated samples were compared at each time point to highlight the time-dependent responses of metabolic profile changes. No or few separations occurred between *F. solani*- and mock-inoculated samples at 0 and 7 dpi (Fig. 2A and B), but a good separation was gradually observed between samples at later time points (Fig. 2C and D). At 21 dpi, mock- and *F. solani*-inoculated samples were clustered independently on the left and right half axes of PC1. PC1 and PC2 accounted for 33.5 and 16.4%, respectively, of the total variance (Fig. 2D). The strong time trend revealed dynamic changes in the AMM metabolism during disease progression.

OPLS-DA was used to maximize the separation between groups and limit the effect of NMR data variation that was unrelated to the sample class. *F. solani*- and mock-inoculated samples were grouped more separately from each other at all the time points on the OPLS-DA score plots (Fig. 3A–D) than on the PCA score plots. Permutation tests were performed to evaluate the validity of the partial least-squares discriminant analysis (PLS-DA) model at 21 dpi. The model exhibited good predictability and goodness of fit for all Q^2 and R^2-values to the left were lower than the original points to the right (Fig. 3E). Thus, the original model was valid at 21 dpi and OPLS-DA could be used to reveal the differential metabolites contributing to the separation between *F. solani*- and mock-inoculated samples at this time point (Fig. 3D). The corresponding scatter plot (S-plot) is displayed in Fig. 3F. The primary metabolites, such as amino acids (*i.e.*, Ala, Arg, Asp, GABA, Gln, Phe, Thr and Val), sugars (*i.e.*, fructose and sucrose), and organic acids (*i.e.*, citric acid, malic acid and taurine), changed significantly and were responsible for the separation of *F. solani*- and mock-inoculated samples ($P < 0.05$, with variable importance in the projection [VIP]>1.0). These metabolites were identified as differential metabolites (Table 2).

Effects of *F. solani* inoculation on the concentration of differential metabolites

ANOVA indicated that the inoculation treatment effects were significant ($P < 0.05$) for the concentration of metabolites, including Ala, Arg, Asp, fructose, Gln, malic

Table 2: Differential metabolites between in *F. solani-* and in mock-inoculated samples

Differential metabolite	VIP	P	
Ala	4.97	1.26×10^{-4}	**
Arg	1.41	0.002	**
Asp	1.47	0.011	*
Citric acid	1.50	0.002	**
Fructose	3.28	2.15×10^{-4}	**
GABA	1.73	0.046	*
Gln	1.06	0.018	*
Malic acid	2.42	9.92×10^{-5}	**
Phe	4.36	2.04×10^{-4}	**
Sucrose	2.37	0.037	*
Taurine	2.58	0.006	**
Thr	1.94	1.25×10^{-7}	**
Val	1.99	1.13×10^{-4}	**

* Significant differences (VIP > 1.0, $P < 0.05$); ** highly significant differences (VIP > 1.0, $P < 0.01$)
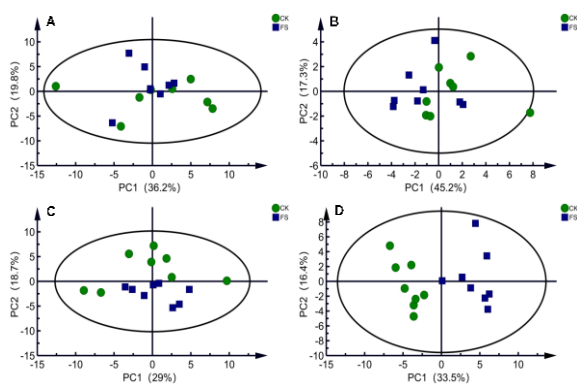
Fig. 2: PCA showing the samples grouping at all-time points after inoculation with *F. solani* or mock. **A-D** represent 0,7,14 and 21 dpi; CK and FS in the figure represent mock- and *F. solani-* inoculated samples, respectively

acid, Phe, sucrose, taurine, and Thr. As shown in Fig. 4, AMM, which was inoculated with *F. solani* or mock, followed a pattern of appearance of metabolites over time. The concentration of Arg increased at 7 and 14 dpi in mock- and *F. solani*-inoculated samples, and then decreased in mock- but remained unchanged in *F. solani*-inoculated samples at 21 dpi. The concentration of Arg in *F. solani*-inoculated samples was significantly lower at 7 dpi and higher at 21 dpi than that in mock-inoculated samples. The concentration of Thr significantly increased in the two treatments at 14 dpi and the change at 21 dpi was the same as that of Arg. The concentration of Gln in mock-inoculated samples increased at 7 dpi and decreased after 14 dpi. However, the concentration of Gln in *F. solani*-inoculated samples increased at 7 dpi, remained unchanged until 21 dpi, and was significantly higher than that in mock-inoculated samples at 14 and 21 dpi. The concentration of Asp increased in both mock- and *F. solani*-inoculated samples at 7 dpi and remained unchanged until 21 dpi. However, the concentration in *F. solani*-inoculated samples increased slowly with a significantly lower concentration at 14 and 21 dpi than that in mock-inoculated ones.
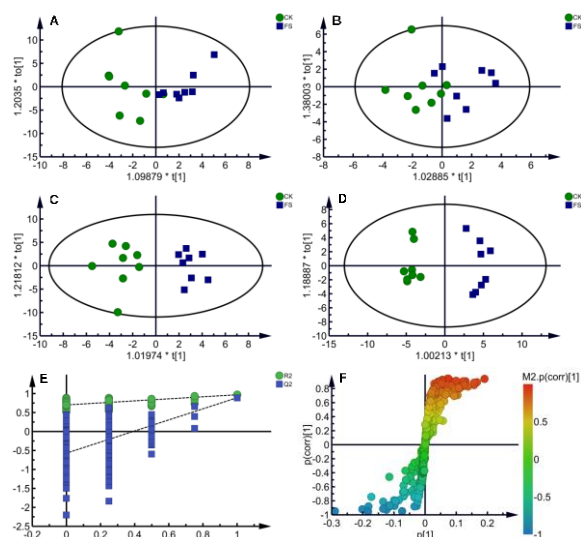
Fig. 3: OPLS-DA showing the samples grouping at all-time points after inoculation with *F. solani* or mock. **A-D** represent 0,7,14 and 21 dpi; **E**: OPLS-DA validation plot at 21 dpi (permutation number: 200); **F**: S-plots corresponding to the OPLS-DA models at 21 dpi; CK and FS in the figure represent mock- and *F. solani*-inoculated samples respectively
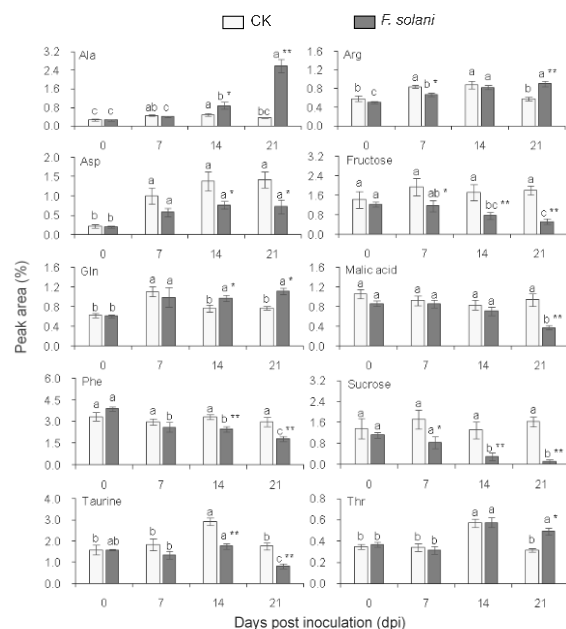
Fig. 4: Relative quantities of metabolites in response to mock and *F. solani* inoculations during the culture process. The different letters represent significant difference at $P < 0.05$ between different time points; *, ** represent the significant difference at $P < 0.05$ and at $P < 0.01$ between *F. solani-* and mock-inoculated samples at each time point; vertical bars represent the standard errors ($n = 8$)

The concentration of Ala increased at 7 dpi in mock-inoculated samples, remained unchanged at 14 dpi, and slightly decreased at 21 dpi. However, the concentration of
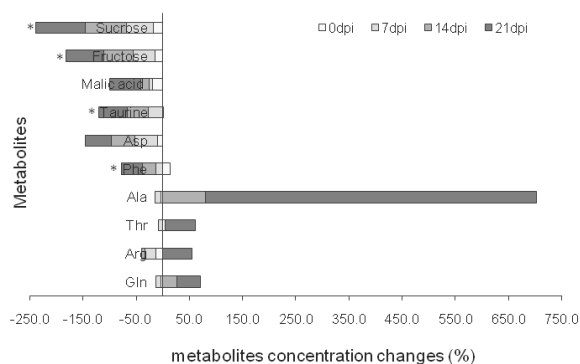
Fig. 5: Metabolite's concentration changes in *F. solani*- and in mock-inoculated samples during the culture process. * indicate significant correlation between concentration changes of metabolites and RRS at $P < 0.05$ level
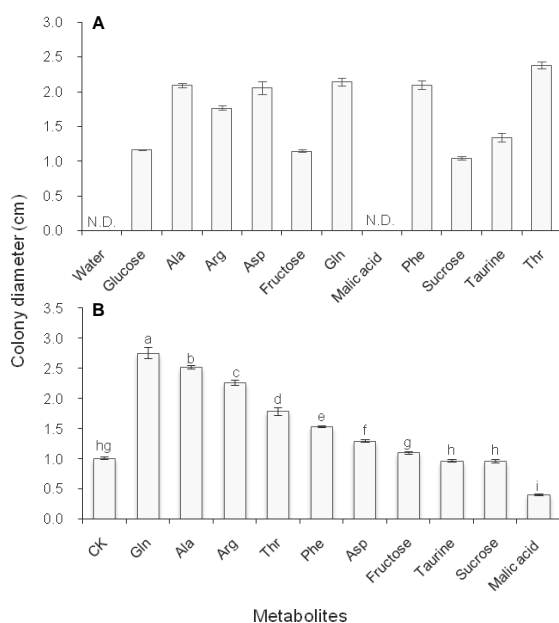

Fig. 6: Effects of differential metabolites on growth of *F. solani* in culture. **A**: Media containing indicated compounds as carbon source; **B**: Media containing glucose and indicated compounds. The different letters represent significant difference at $P < 0.05$; vertical bars represent standard errors ($n = 5$)

Ala in *F. solani*-inoculated samples gradually increased and reached a particularly high concentration at 21 dpi. Phe showed no evident change after the mock challenge but reduced with time after inoculation with *F. solani*, showing significantly low accumulation at 14 and 21 dpi. The concentrations of fructose and sucrose in *F. solani*-inoculated samples showed a significant decline with time and exhibited significantly low accumulation at 7, 14 and 21 dpi. No clear change in amount was found in mock-inoculated samples. The change in the pattern of malic acid in *F. solani*-inoculated samples was similar to that of Phe, with the significant decrease appearing at 21 dpi, but no

significant difference was found between each time points in the control. The concentration of taurine in mock- and *F. solani*-inoculated samples reached its peak at 14 dpi and decreased at 21 dpi. The concentration of taurine in *F. solani*-inoculated samples was clearly lower than that in mock-inoculated samples at 14 and 21 dpi.

RR and PR metabolites

Of the 10 differential metabolites with significant concentration change in response to the challenge of *F. solani*, the ratio of concentration reduction of sucrose, fructose, Asp, Phe, malic acid, and taurine had an increasing trend with increasing RRS; while the ratio of concentration growth of other four metabolites had an increasing trend with increasing RRS (Fig. 5). These changes suggested that several of these differential metabolites might have substantially positive or negative correlations with the disease development. The Pearson correlation analysis over all time points showed that the concentration changes in Phe ($r = -0.952$, $p = 0.048$), fructose ($r = -0.966$, $p = 0.034$), sucrose ($r = -0.976$, $p = 0.024$) and taurine ($r = -0.956$, $p = 0.044$), had a significantly negative correlation with RRS (Fig. 5). Among other differential metabolites, none was found to have strong correlations, but Asp and malic acid showed significant decreases with the infection process. Asp exhibited evident relative change in concentration at 14 and 21 dpi and the Asp concentrations in *F. solani*-inoculated samples were lower by 44.09% and 48.94%, respectively, than those in mock-inoculated samples. Malic acid exhibited a significant decrease in concentration by 59.52% at 21 dpi. In accordance with the criteria for identifying the RR and PR metabolites, Phe, Asp, fructose, sucrose, taurine, and malic acid were potential RR metabolites, whereas Ala, Arg, Gln and Thr, were potential PR metabolites.

Effects of selected metabolites on the *F. solani* growth

Compounds that were identified as potential RR (Phe, Asp, fructose, sucrose, taurine, and malic acid) or PR metabolites (Ala, Arg, Gln and Thr) were tested for their effects on *F. solani* growth. *F. solani* was found to use Ala, Arg, Asp, fructose, Gln, Phe, sucrose, taurine and Thr as carbon sources (Fig. 6A), but no growth was observed when malic acid was provided. Supplementation with Ala, Arg, Asp, Gln, Phe, and Thr enhanced fungal growth. Malic acid supplementation inhibited growth, and fructose, sucrose, and taurine supplementation had no effect (Fig. 6B).

Discussion

Resistant cultivars can counteract pathogen infection and spread by implementing multiple defense strategies in different biochemical pathways involved in primary and secondary metabolism. In this study, we found that *F. solani* inoculation had marked effects on the AMM primary

metabolite level, including amino acid, sugar, and organic carboxylic acids. Several metabolites were identified as RR metabolites. Results indicated that AMM might mount defense mechanisms by reorganizing the primary metabolism or activating/regulating secondary disease-resistant metabolic pathways involved with selected RR metabolites.

Studies showed that amino acids are crucial in the signaling of interaction between plants and compatible pathogens (Sétamou *et al.* 2017). Fungi derive amino acids from plants by recycling or via proteolysis (Solomon *et al.* 2003). The strong demand of plants to obtain carbon likely transports amino acids into energy-generating pathways, such as the TCA cycle (Bolton 2009) and may mobilize some nitrogen sources, such as nitrogen-rich amino acids, away from infection sites to take away nutrients from pathogen (Tavernier *et al.* 2007). In our study, with prolonged inoculation time and increased RRS, amino acid fluctuations could be grouped into downregulated (Asp and Phe) and upregulated (Ala, Arg, Gln and Thr) fluctuations. The different temporal fluctuations of amino acids might show differential requirements for amino acid on the part of *F. solani* during infection process or on the part of the plant during defense responses.

Phe, as the precursor of many RR metabolites (*i.e.*, lignins, 4-coumaric acid, and cinnamic acid) of the phenylpropanoid pathway (Dixon 2001), can contribute to the plant resistance to pathogen infection. When plants are attacked by pathogens, the phenylalanine ammonia lyase (PAL), which is well known to be induced after fungal infections, may deplete Phe in producing defense compounds, such as lignin (Cuperlovic-Culf *et al.* 2016). This condition might be one of the reasons why the Phe concentration decreased with the expansion of pathogens in AMM. Simultaneously, the concentration changes in Phe had a negative correlation with the RRS. This condition might imply that the lack of Phe resulted in the reduction in other related antifungal substances synthesized in the phenylpropanoid pathway, leading to the increasing RRS of AMM. Research showed significant Phe abundance differences between resistant and susceptible lines (Cuperlovic-Culf *et al.* 2016). Kumaraswamy *et al.* (2011a) found that Phe in some barley-resistant genotypes showed a twofold or higher abundance than that in susceptible ones. Turetschek *et al.* (2017) reported that Phe depletes significantly in the susceptible field pea cv. *Messire* against *Didymella pinodes*. By contrast, the tolerant cv. *Protecta* manages to preserve its Phe levels. Considering the above analysis and test results, Phe was identified as an RR metabolite and could be used as a candidate biomarker for AMM against *F. solani* infection. Interestingly, Phe evidently enhanced the *F. solani* mycelial growth, indicating that Phe contributed more to improving plant defense than to enhancing pathogen growth in the AMM–*F. solani* pathogenesis. However, the coordination of the two mechanisms remains unknown.

In many higher plants, the nitrogen rich Gln represents the central intermediates in nitrogen because it helps bring about nitrogen transport, and its encoding genes are upregulated under biotic stresses (Copley *et al.* 2017). As the main nitrogen donor for amino acid synthesis, Gln may provide a major source of nitrogen for protein synthesis in growing hyphae (Parker *et al.* 2009). In our study, the concentration of Gln increased with time after *F. solani* challenge and the effect of significant promotion on mycelial growth was found. This condition might suggest that as the infection was established, *F. solani* could manipulate AMM's metabolism to promote the production of Gln. Gln was utilized downstream and promoted the growth and expansion of *F. solani* in AMM. Similar findings on Gln increase were reported on soybeans infected with *Rhizoctonia solani* (Copley *et al.* 2017) and rice infected with compatible *Magnoportha grisea* (Jones *et al.* 2011). These results provided some pieces of evidence to support our assumption of Gln as PR metabolites.

The easy conversion from Asp to Glu, from which Gln is derived, may provide an additional source of translocated nitrogen for the growing pathogen (Parker *et al.* 2009). We found that compared with the control, the infected AMM had decreased Asp concentration and increased Gln concentration at 14 dpi and 21 dpi. These data suggested that AMM with a high Asp concentration might imply that its level of Gln would increase easily when infected by *F. solani*, which might accelerate the spread of *F. solani* root rot. Hence, Asp was not considered an RR metabolite in our research.

However, Gln showed evidently increased abundances in susceptible and resistant wheat cultivars inoculated with *F. graminearum*, and more increase was observed in the latter. A high abundance of Gln, which helps the plant cell recycle liberated ammonia ions from Phe, can be an evidence of an active PAL pathway and phenylpropanoid metabolism in the resistant cultivar (Hamzehzarghani *et al.* 2005).

The Ala levels in *F. solani*-inoculated samples increased by 80.15% and 622.57% at 14 and 21 dpi, respectively. Marked accumulations of Ala are found in rice infected with compatible *M. grisea* (Jones *et al.* 2011), healthy and botrytized berries of grape bunches infected with *Botrytis cinerea* (Hong *et al.* 2012), and soybean infected with *R. solani* (Copley *et al.* 2017). Ala participates in the activation of programmed cell death response in suspension cultures of Concord grape (*Vitis labrusca*) (Chen *et al.* 2006). The successful invasion of *F. solani* triggering an increase in Ala concentration possibly promotes the cell death of the infected AMM tissue, which *F. solani* then exploits to facilitate invasion. Simultaneously, Ala significantly enhanced the fungal growth in the present study. Although the above analysis supported our conclusion that Ala can be considered a PR metabolite, several studies reported the constitutive accumulation of Ala in grapevine cultivars resistant to fungal infection, illustrating its protective action on biotic stresses (Lima *et*

al. 2010). Ala synthesis increases to regulate cellular osmosis that is decreased by high cellular carbohydrate levels under anaerobic or hypoxic conditions in diseased plants (Hong *et al.* 2012).

Arg and Thr showed significantly high accumulation in inoculation samples at 21 dpi and supplementation with Thr and Arg had positive effects on the active growth of *F. solani*. Arg and Thr were identified as PR metabolites in the present study. The increase in Arg is considered a general feature of pathogenesis (Solomon *et al.* 2003). This amino acid can serve as a major storage and transport form of organic nitrogen (especially during biotic and abiotic stresses in plants) and a potential nitrogen and energy substrates for many microorganisms, such as bacteria within plants (Sétamou *et al.* 2017). Thus, Arg was likely to enhance *F. solani* mycelial growth by providing the substrate of energy metabolism or substance synthesis, thereby accelerating the enlargement in root rot disease. However, Arg is identified as an RR metabolite in barley against FHB because it can act as a precursor for the biosynthesis of a polyamine, which is involved in various stress responses (Bollina *et al.* 2010). The significant accumulation of Thr is observed in the skin and pulp of the healthy berries of botrytized grape bunches infected by *B. cinerea* compared with those of healthy grape bunches. The increased levels of Thr are speculated to result from elevated amino acid synthesis of plant host during an active synthesis of cell wall constituents in response to *B. cinerea* infection. The accumulation of Thr concentration also indicates its role as a nitrogen source for the active growth of *B. cinerea* (Hong *et al.* 2012). In the present study, Thr might have similar action mechanism in AMM challenged with *F. solani*.

Sugars, including sucrose, glucose, fructose, and maltose, are the main source of energy for the growth and development of cellular machinery. The abnormality of sugar content or concentration may lead to abnormal glucose metabolism. Sucrose acts as a major source of carbon in many physiological processes, such as growth, development, and response to a variety of stresses (Naseem *et al.* 2017). Pathogens have formed diverse strategies to compete with their hosts for sucrose (Wahl *et al.* 2010). Fructose, the byproduct of sucrose, is less competitive than glucose for microbial nutrition. However, increasing evidence implies that pathogen infection results in the release of free hexoses (*i.e.*, fructose) that provide nourishment to apoplast-adopted pathogens (Naseem *et al.* 2017). Therefore, one of the reasons why the contents of sucrose and fructose in AMM constantly decrease after the *F. solani* inoculation might be the consumption of sugar by pathogens. The results that fructose and sucrose can be utilized by *F. solani* as carbon sources provided evidence for the above assumption.

Considering that the sugar availability for the pathogen plays a pivotal role during infection, a simple and direct way for the host to control microbial density is limiting the access to nutrients and activating the immune system. Plants deploy many mechanisms to regulate carbon fluxes in the apoplastic space, in which many pathogens live or at least grow at a certain phase (Oliva and Quibod 2017). Studies showed that sugar concentrations remain high until the end of infection during a tolerant defense response (Joosten *et al.* 1990). The accumulation of sugar in tolerant pea may indicate high tolerance and slow infection because sugars are not metabolized by the pathogen (Turetschek *et al.* 2017). The increase in sugar concentrations in high-resistance wheat variety Sumai3 and moderate-resistance variety FL62R1 suggest an attempt at the creation of cell wall barrier for *F. graminearum* invasion (Cuperlovic-Culf *et al.* 2016). The metabolic profiling of wheat spikelets displays high abundance of several metabolites putatively identified as sugars, which may help elucidate wheat resistance to *F. graminearum*. The abundances of fructose in some resistant genotypes are higher than that in susceptible genotypes (Hamzehzarghani *et al.* 2005). Glucose, fructose, galactose, and sucrose in *F. verticillioides*-resistant inbred maize exhibited higher levels compared with those in *F. verticillioides*-susceptible inbred maize (Campos-Bermudez *et al.* 2013). The above information supported our findings that sucrose and fructose were RR metabolites and could be selected as candidate biomarkers for discriminating the resistance levels of AMM.

Organic carboxylic acids are substrates for the synthesis of various amino acids and are the connecting point for the metabolism of various substances in plants. The malic acid content is directly related to plant growth, development, and resistance (Dong *et al.* 2015). Malic acid has antimicrobial activity (Xue *et al.* 2004) and considered an important RR metabolite in wheat against FHB (Hamzehzarghani *et al.* 2008). The significant reduction in malic acid in *F. solani*-inoculated samples was observed at 21 dpi and the change was consistent with that in banana roots infected by *F. oxysporum* (Dong *et al.* 2015). Malic acid cannot be utilized as a carbon source by *F. solani* and strongly inhibited the mycelial growth. The reduction in malic acid might indicate a decrease in the resistance of AMM to *F. solani* infection or the weakened ability to inhibit *F. solani* mycelial spread in plant tissue. This condition resulted in the aggravation of diseases. Taurine is an important nutrient that regulates the normal physiological functions of animal bodies. Taurine protects biological cells, maintains the stability of cell membranes, and protects the activity of antioxidant enzyme systems (Hao *et al.* 2004). However, few reports are available about the function of taurine involved with plant defense responses against pathogens. A related example is that the accumulation level of taurine in rice-resistant cultivars (IR56) notably increases during brown planthopper (BPH) infestation and may work to reduce the ROS-induced oxidative pressure caused by BPH feeding (Kang *et al.* 2019). Another report showed that the cell membrane relative permeability and the content of malondialdehyde, a product of membrane lipid peroxidation, decreases when wheat seedlings are grown in

taurine solution, suggesting that taurine protects the cell membrane of wheat (Hao *et al.* 2004). Thus, the decrease in taurine concentration in AMM might weaken the abilities in balancing the level changes in ROS and lowering the degree of cell membrane lipid peroxidation. The two phenomena could be caused by *F. solani* infection. Therefore, malic acid and taurine were considered RR metabolites and selected as candidate resistance biomarkers in AMM.

As is shown in the above discussion, some reports regarding the antifungal mechanism of metabolites support our assumption that the selected RR metabolites can serve as resistance metabolic biomarkers in the AMM–*F. solani* pathogenesis. However, the changes in the metabolic profiling that we observed might vary in response to different pathogens and hosts, and the function of various metabolites might change in a concerted fashion. Besides, the production or change in the metabolites in plant could be induced by a series of stresses, such as temperature and drought. Thus, the verification of function and mechanism of these RR metabolites in the disease-resistant metabolic pathway must be conducted in the future to further assess their suitability as biomarkers.

The metabolomics approach enables the visualization of some metabolites of the plant–pathogen interaction and contributes to an improved understanding of the functions of metabolites. Metabolites are linked to specific genomic positions, and a set of colocalized genes regulate certain metabolic pathways through a series of enzymatic reactions, resulting in the production of a series of metabolites, which are linked to phenotypes (Hamzehzarghani *et al.* 2008). Therefore, combined with other omics, metabolomics can provide opportunities for AMM disease-resistant breeding through the identification of RR metabolites that can assist in the selection of suitable/required resistance genes for breeding.

In addition, only a small number of metabolites are identified, and most of them belong to primary metabolites in the present study. The improvement of the metabolomics protocol, such as optimizing the sample extraction procedure, analyzing the organic fractions of the sample extracts, and using 2D-NMR and LC–MS, is beneficial to the revelation of more metabolites especially secondary metabolites that might relate to the resistance mechanisms of AMM to *F. solani*.

Conclusion

This study first reported the changes in metabolite profiling in AMM plants infected by the root rot pathogen *F. solani* especially the levels of primary metabolites, including amino acid, sugar and organic carboxylic acids. Of the 24 metabolites examined, Phe, sucrose, fructose, malic acid, and taurine were identified as RR metabolites and likely to serve as candidate biomarkers for discriminating the resistance levels of AMM genotypes and establishing high-throughput screening method of AMM breeding lines

against the root rot caused by *F. solani*.

Author Contributions

Fen Gao conceived the idea, designed the experiments, and wrote the paper. Jianbin Chao and Jie Guo conducted the NMR analysis. Li Zhao analyzed the data. Haijiao Tian did other experimental work. All authors read and approved the manuscript.

Conflict of Interest

The authors declare that there is no conflict of interest regarding the publication of the manuscript.

Data Availability

The data will be made available on fair request to the corresponding author.

Ethics Approval

Not applicable.

References

Bollina V, AC Kushalappa, TM Choo, Y Dion, S Rioux (2011). Identification of metabolites related to mechanisms of resistance in barley against *Fusarium graminearum* based on mass spectrometry. *Plant Mol Biol* 77:355–370

Bollina V, KG Kumaraswamy, AC Kushalappa, TM Choo, Y Dion, S Rioux, D Faubert, H Hamzehzarghani (2010). Mass spectrometry-based metabolomics application to identify quantitative resistance related metabolites in barley against *Fusarium* head blight. *Mol Plant Pathol* 11:769–782

Bolton MD (2009). Primary metabolism and plant defense-fuel for the fire. *Mol Plant Microb Interact* 22:487–97

Botanga CJ, G Bethke, Z Chen, DR Gallie, O Fiehn, J Glazebrook (2012). Metabolite profiling of *Arabidopsis* inoculated with *Alternaria brassicicola* reveals that ascorbate reduces disease severity. *Mol Plant Microb Interact* 25:1628–1638

Campos-Bermudez VA, CM Fauguel, MA Tronconi, P Casati, DA Presello, CS Andreo (2013). Transcriptional and metabolic changes associated to the infection by *Fusarium verticillioides* in maize inbreds with contrasting Ear Rot resistance. *PLoS One* 8; Article e61580

Chen JX, DE Hall, J Murata, VD Luca (2006). L-Alanine induces programmed cell death in *V. labrusca* cell suspension cultures. *Plant Sci* 171:734–744

Copley TR, KA Aliferis, DJ Kliebenstein, SH Jabaji (2017). An integrated RNA seq-^{1}H NMR metabolomics approach to understand soybean primary metabolism regulation in response to *Rhizoctonia* foliar blight disease. *BMC Plant Biol* 17; Article 84

Cuperlovic-Culf M, L Wang, L Forseille, K Boyle, N Merkley, I Burton, PR Fobert (2016). Metabolic biomarker panels of response to Fusarium head blight infection in different wheat varieties. *PLoS One* 11; Article e0153642

Dixon RA (2001). Natural products and plant disease resistance. *Nature* 411:843–847

Dong X, QS Zheng, M Wang, JY Zhou, QR Shen, SW Guo (2015). Physiological response of three types of organic small molecule solutes in banana seedlings to *Fusarium oxysporum* infection. *Acta Ecol Sin* 35:3309–3319

Gao F, XX Zhao, XM Qin, ZH Lei (2018). Analysis of dominant pathogen community causing *Astragalus membranaceus* var. *mongholicus* root rot in Shanxi Province. *J Plant Prot* 45:878–885

Gauthier L, V Atanasova-Penichon, S Chéreau, F Richard-Forget (2015). Metabolomics to decipher the chemical defense of cereals against *Fusarium graminearum* and deoxynivalenol accumulation. *Intl J Mol Sci* 16:24839–24872

Hamzehzarghani H, V Paranidharan, Y Abu-Nada, AC Kushalappa, Y Dion, S Rioux, A Comeau, V Yaylayan, WD Marshall (2008). Metabolite profiling coupled with statistical analyses for potential high throughput screening of quantitative resistance to *Fusarium* head blight in wheat. *Can J Plant Pathol* 30:24–36

Hamzehzarghani H, AC Kushalappa, Y Dion, S Rioux, A Comeau, V Yaylayan, WD Marshall, DE Mather (2005). Metabolic profiling and factor analysis to discriminate quantitative resistance in wheat cultivars against Fusarium head blight. *Physiol Mol Plant Pathol* 66:119–133

Hao LH, PQ He, CY Liu, KS Chen, GY Li (2004). Physiological effects of taurine on the growth of wheat (*Triticum aestivum* L.) seedlings. *J Plant Physiol Mol Biol* 30:595–598

He P, ZY Li, SC Fan, FS Zhang, XM Qin, GJ Du (2013). Differences between Hengshanhuangqi and Chuanhuangqi based on metabolomics and ITS2 sequences. *Acta Pharm Sin* 48:1595–1601

Hong YS, A Martinez, G Liger-Belair, P Jeandet, JM Nuzillard, C Cilindre (2012). Metabolomics reveals simultaneous influences of plant defence system and fungal growth in *Botrytis cinerea* infected *Vitis vinifera* cv. chardonnay berries. *J Exp Bot* 63:5773–5785

Iqbal SM, A Javaid, A Bakhsh, SR Malik (2013). Molecular characterization of pea for resistance to *Pseudomonas syringae* pv. *pisi*. *Intl J Agric Biol* 15:787–790

Jones OAH, ML Maguire, JL Griffin, YH Jung, J Shibato, R Rakwal, GK Agrawal, NS Jwa (2011). Using metabolic profiling to assess plant-pathogen interactions: an example using rice (*Oryza sativa*) and the blast pathogen *Magnaporthe grisea*. *Eur J Plant Pathol* 129:539–554

Joosten MHAJ, LJM Hendrickx, PJGM Dewit (1990). Carbohydrate-composition of apoplastic fluids isolated from tomato leaves inoculated with virulent or avirulent races of *Cladosporium fulvum* (Syn *Fulvia fulva*). *Neth J Plant Pathol* 96:103–112

Kang K, L Yue, X Xia, K Liu, W Zhang (2019). Comparative metabolomics analysis of different resistant rice varieties in response to the brown planthopper *Nilaparvata lugens* Hemiptera: Delphacidae. *Metabolomics* 15; Article 62

Kumaraswamy KG, AC Kushalappa, TM Choo, Y Dion, S Rioux (2011a). Mass spectrometry based metabolomics to identify potential biomarkers for resistance in barley against Fusarium head blight (*Fusarium graminearum*). *J Chem Ecol* 37:846–856

Kumaraswamy KG, V Bollina, AC Kushalappa, TM Choo, Y Dion, S Rioux, O Mamer, D Faubert (2011b). Metabolomics technology to phenotype resistance in barley against *Gibberella zeae*. *Eur J Plant Pathol* 130:29–43

Li AP, ZY Li, TL Qu, XM Qin, GH Du (2017). Nuclear magnetic resonance based metabolomic differentiation of different *Astragali Radix*. *Chin J Nat Med* 15:363–374

Li AP, ZY Li, HF Sun, K Li, XM Qin, GH Du (2015). Comparison of two different *Astragali Radix* by a ^{1}H NMR-based metabolomic approach. *J Proteom Res* 14:2005–2016

Li SD, ZQ Miao, WD Gao (2011). Challenges, opportunities and obligations in management of soilborne plant diseases in China. *Chin J Biol Cont* 4:433–440

Lima MRM, ML Felgueiras, G Graça, JEA Rodrigues, A Barros, AM Gil, ACP Dias (2010). NMR metabolomics of esca disease-affected *Vitis vinifera* cv. *Alvarinho* leaves. *J Exp Bot* 61:4033–4042

Ma YY, YM Guan, QX Wang, MJ Li, XX Pan, YY Zhang (2019). Research progress on main diseases and control measures of *Astragalus membranaceus*. *Spec Wild Econ Anim Plant Res* 4:101–107

Naseem M, M Kunz, T Dandekar (2017). Plant-pathogen maneuvering over apoplastic sugars. *Trends Plant Sci* 22:740–743

Oliva R, IL Quibod (2017). Immunity and starvation: new opportunities to elevate disease resistance in crops. *Curr Opin Plant Biol* 38:84–91

Parker D, M Beckmann, H Zubair, DP Enot1, Z Caracuel-Rios, DP Overy, S Snowdon, NJ Talbot, J Draper (2009). Metabolic analysis reveals a common pattern of metabolic re-programming during invasion of three host plant species by *Magnaporthe grisea*. *Plant J* 59:723–737

Qin XM, L Aip, K Li, L AnP, LH Ning (2016). Thinking on development of Shanxi *Astragali radix* industry. *Chin J Chin Mater Med* 24:4670–4674

Sétamou M, OJ Alabi, CR Simpson, JL Jifon (2017). Contrasting amino acid profiles among permissive and non-permissive hosts of *Candidatus Liberibacter asiaticus*, putative causal agent of Huanglongbing. *PLoS One* 12; Article e0187921

Solomon PS, KC Tan, RP Oliver (2003). The nutrient supply of pathogenic fungi: a fertile field for study. *Mol Plant Pathol* 4:203–210

Tavernier V, S Cadiou, K Pageau, R Laugé, M Reisdorf-Cren, T Langin, C Masclaux-Daubresse (2007). The plant nitrogen mobilization promoted by *Colletotrichum lindemuthianum* in phaseolus leaves depends on fungus pathogenicity. *J Exp Bot* 58:3351–3360

Turetschek R, G Desalegn, T Epple, HP Kaul, S Wienkoop (2017). Key metabolic traits of *Pisumsativum* maintain cell vitality during *Didymella pinodes* infection: cultivar resistance and the microsymbionts' influence. *J Proteom* 169:189–201

Wahl R, K Wippel, S Goos, J Kämper, N Sauer (2010). A novel high-affinity sucrose transporter is required for virulence of the plant pathogen *Ustilago maydis*. *PLoS Biol* 8; Article e1000303

Xue JJ, CQ Fan, L Dong, SP Yang, JM Yue (2004). Novel antibacterial diterpenoids from *Larix chinensis* Beissn. *Chem Biodivers* 1:1702–1707